

# Magnetic fluids in an external field

 F. Schinagl<sup>1</sup>, H. Iro<sup>2</sup> and R. Folk<sup>2,a</sup>
<sup>1</sup> Institute for Semiconductor Physics, University of Linz, Altenbergerstrasse 69, 4040 Linz, Austria

<sup>2</sup> Institute for Theoretical Physics, University of Linz, Altenbergerstrasse 69, 4040 Linz, Austria

Received 20 March 1998

**Abstract.** Within mean field approximation we investigate the phase diagrams of magnetic fluids in presence of a magnetic field. In a finite field the magnetic phase transition is absent, but instead a line of first order liquid-liquid transitions ending in a critical point occurs for a magnetic interaction, which is sufficiently strong. Varying the magnetic field these critical points extend from the tricritical point at  $H = 0$  to a critical endpoint. For a fluid with Ising spins we calculate the critical lines and several tricritical exponents analytically. For Heisenberg fluids we obtain the phase diagrams from a numerical solution of the mean field equations of state.

**PACS.** 64.60.Fr Equilibrium properties near critical points, critical exponents – 64.60.Kw Multicritical points – 75.50.Mm Magnetic liquids

## 1 Introduction

So far liquid ferromagnetism has been verified in colloidal systems, *e.g.* Au–Co alloys [1,2]. Moreover it is now well-established by computer simulations that a fluid of particles, which carry spin (Ising or Heisenberg type) and interact via a short range magnetic force, may arrange itself in a ferromagnetic liquid phase [3–12]. Depending on the relative strengths of the magnetic interaction and the non-magnetic interaction the magnetic phase, the gaseous phase and the liquid phase may form phase diagrams of different topologies containing first and second order phase transition lines ending in critical or tricritical points [13,14]. Since so far most of the interest was focused on the magnetic phase transition, the phase diagrams were studied for magnetic field  $H$  equal to zero. Continuing the work of references [13,14] we extend the mean field phase diagrams to non-zero magnetic fields. We think that a complete exploitation of the phase diagrams based on the mean field equations of state is a valuable reference for real as well as for computer experiments. Although in a magnetic field no magnetic transition exists, an additional liquid-liquid transition may be present forming the wings related to the tricritical point at  $H = 0$ . If the gas-liquid transition surface is present, its intersection with these wings leads to a line of triple points terminating in a critical end point.

A number of models exhibiting tricritical points are known [15], most of them are lattice models or models for mixtures (*e.g.* <sup>3</sup>He–<sup>4</sup>He). In many magnetic models it is the competition of ferromagnetic and antiferromagnetic

ordering which leads to multicritical behavior. In magnetic liquids, a one component system, it is the competition between magnetic and spatial (density) ordering which leads to multicriticality. The phase diagrams in the space of pressure, temperature and magnetic field are symmetric with respect to the magnetic field. Therefore in mean field theory, concerning the tricritical behavior classical critical exponents of symmetric type are found.

The magnetic liquid is another interesting model system for studying multicritical behavior without using Landau expansion. For a van der Waals gas whose particles carry in addition Ising spins certain phase transition lines can be calculated analytically.

## 2 The one-dimensional Ising fluid

There are two coupled equations of state for a magnetic van der Waals gas of hard spheres (with diameter  $b$ ): one fixing mainly the magnetic properties and the other governing the density (fluid) degrees of freedom. In mean field approximation these equations are given *e.g.* in references [13,14]. As equation of state (EOS) ruling the magnetic properties we take the mean-field equation of an Ising system (see [14])

$$m(\rho, T, H) = \tanh \frac{a_m \rho m + H}{k_B T}, \quad (2.1)$$

rendering the magnetization  $m$  as function of the particle-density  $\rho$ , the temperature  $T$  and the magnetic field  $H$ .  $a_m$  is a measure of the strength of the magnetic interaction. The equation of state for the pressure  $P$  of the system is

---

<sup>a</sup> e-mail: folk@tphys.uni-linz.ac.at

the modified van der Waals equation

$$P(\rho, T, m^2) = \mathcal{MC} \left( k_B T \frac{\rho}{1 - b\rho} - \frac{1}{2} a_m m^2 \rho^2 - \frac{1}{2} a \rho^2 \right) \quad (2.2)$$

where in addition to the attractive interaction of strength  $a$  the magnetic interaction appears. The hard core repulsion restricts the density to  $\rho > b$ . In (2.2) for nonmonotonic isotherms the Maxwell construction has to be performed; this is indicated by  $\mathcal{MC}$ . It is convenient to introduce the reduced variables

$$x = \frac{1}{\rho b}, \quad t = \frac{k_B T b}{a}, \quad h = H b / a$$

$$p = p(x, t, m^2) = \frac{b^2}{a} P(\rho, T, m^2). \quad (2.3)$$

Then only the ratio  $R = a_m / a$  of the magnetic to the van der Waals interaction remains as parameter in the equations of state

$$m = \tanh \left( \frac{Rm}{xt} + \frac{h}{t} \right) \quad (2.4)$$

$$p = \mathcal{MC} \left( \frac{t}{x-1} - R \frac{m^2}{2x^2} - \frac{1}{2x^2} \right). \quad (2.5)$$

Depending on  $R$  several topologies of phase diagrams occur.

## 2.1 Short summary of the critical behavior for $H = 0$

### 2.1.1 The magnetic phase transition

The magnetic equation of state  $m(x, t) = \tanh(Rm/xt)$  shows that magnetic phase transitions take place for values  $t_m, x_m$  on the line

$$x_m t_m / R = 1. \quad (2.6)$$

These transitions are of second order as long as the compressibility is larger than zero, *i.e.*  $\partial p / \partial x|_{x_m t_m \rightarrow R_-} \geq 0$ . Given a fixed value of  $x_m$ , the fluid is paramagnetic in the high-temperature region, whereas it becomes ferromagnetic for temperatures below  $t_m$ ; the order parameter is the spontaneous magnetization  $m_0$ , *i.e.* the solution of (2.4) at  $h = 0$ :  $m_0 = \tanh(Rm_0/xt)$ . For  $xt/R \rightarrow 1_-$  the magnetization  $m_0$  is approximately

$$m_0^2 \simeq 3(1 - xt/R), \quad (2.7)$$

so that the critical exponent  $\beta$  assumes its mean field value  $1/2$ .

In the  $(t, p)$ -plane the transition points  $(t_m, p_m)$  form the line  $L_\lambda$

$$p_m = t_m^2 \left( \frac{1}{R - t_m} - \frac{1}{2R^2} \right). \quad (2.8)$$

This line ceases to be physically relevant in the tricritical point (TCP) at  $x = x_t$  with temperature and pressure  $(t_t, p_t)$ . For the tricritical temperature the isotherm in the  $p - x$  diagram has zero slope approaching the transition line from the ferromagnetic phase [13]

$$\left. \frac{\partial p}{\partial x} \right|_{t \rightarrow t_{m,-}} = 0; \quad (2.9)$$

together with (2.7) and  $xt = R$  this condition yields the values for temperature and pressure at the tricritical point

$$t_t = R \left( 1 - \sqrt{\frac{2R}{3R+2}} \right),$$

$$p_t = \left( 1 - \sqrt{\frac{2R}{3R+2}} \right)^2 \left( \frac{R}{\sqrt{\frac{2R}{3R+2}}} - \frac{1}{2} \right) \quad (2.10)$$

and  $x_t = \frac{(3R+2)}{R+2} \left( 1 + \sqrt{\frac{2R}{3R+2}} \right)$  (observe that  $x_t = R/t_t \geq 1$ ).

In the vicinity of the tricritical point the exponent  $\beta_t$  describes the behavior of the magnetization approaching the tricritical point at constant  $t_t$  along the line  $p \rightarrow p_{t+}$  [15,16]. Using (2.7) in (2.5) and observing that near the tricritical point the compressibility vanishes in the ordered phase (2.9) one can check that  $\beta_t = 1/4$ . Below the tricritical point there is a first order phase transition line  $L_\tau$  in the  $(t, p)$ -diagram separating a paramagnetic fluid phase from a ferromagnetic fluid phase (this line can be obtained by a Maxwell construction). Since the magnetization is coupled to the density, the jump in  $m$  induces a jump in  $x$ .

### 2.1.2 The gas-liquid phase transition

For  $m = 0$ , *i.e.*  $xt > R$ , there may exist also the critical point (CP) of the nonmagnetic van der Waals gas ( $\partial p / \partial x = \partial^2 p / \partial x^2 = 0$ ), at the well known values

$$t_c = \frac{4}{27}, \quad p_c = \frac{1}{54} \quad (2.11)$$

and  $x_c = 3$ . The order parameter is the volume (density) of the gas. For  $t < t_c$  there are then first order transitions from the gas to the liquid phase; both are paramagnetic. One finds (see Ref. [17], p. 52)  $|x_c - x| \propto (p_c - p)^{1/2}$  for  $t = t_c$  and  $|x_{c1} - x_{c2}| \propto |t_c - t|^{1/2}$  for  $p = p_c$  so that for this transition also  $\beta = 1/2$ . But this critical point is only present if at least  $t_c x_c = 4/9 > R$ . To find out the actual range of existence of this critical point one has to consider the first order phase transition lines of the magnetic and the gas-liquid transition. These meet in a triple point. Varying  $R$ , two types of phase diagrams exist. Either the first order line of the magnetic transition may become shorter and shorter, so that in the limiting case the tricritical point becomes a critical end point (CEP) on the first order gas-liquid transition line, or the first order

gas-liquid transition line becomes shorter and shorter and the gas-liquid critical point disappears. In the latter case only a magnetic transition line consisting of a second order transition part separated by the tricritical point from the first order transition part exists. According to reference [14] the first situation occurs for  $R \leq R_1 \simeq 0.211$ , whereas the second one for  $R \geq R_2 \simeq 0.304$ .

## 2.2 The ideal Ising fluid of rigid spheres

We first investigate a simplified model by switching off the nonmagnetic part of the interaction, *i.e.* we set  $a = 0$ . Then only magnetically induced phase transitions in the fluid phase remain. Nevertheless the phase diagram of this model exhibits a tricritical point.

To obtain this limit of a gas of rigid spheres from the equations of state (2.4, 2.5) one has first to rescale the fields according to

$$\bar{p} = p/R, \quad \bar{t} = t/R, \quad \bar{h} = h/R.$$

Then performing the limit  $R \rightarrow \infty$  yields

$$m = \tanh \left( \frac{m}{x\bar{t}} + \frac{\bar{h}}{\bar{t}} \right) \quad (2.12)$$

$$\bar{p} = \frac{\bar{t}}{x-1} - \frac{m^2}{2x^2}. \quad (2.13)$$

### 2.2.1 The critical behavior in zero magnetic field

For  $\bar{h} = 0$  the variety of phase diagrams mentioned above is reduced. Only the topology without a gas liquid transition (within the complete model it is found for parameter values  $R > 0.304$ ), remains. There is only the line of second order magnetic transitions for

$$\bar{t}_m x_m = 1 \quad (2.14)$$

which terminates in the tricritical point

$$\begin{aligned} \bar{t}_t &= 1 - \sqrt{\frac{2}{3}} = 0.184, \\ \bar{p}_t &= \frac{5}{2} \sqrt{\frac{2}{3}} - 2 = 4.124 \times 10^{-2} \end{aligned} \quad (2.15)$$

and  $x_t = 3 + \sqrt{6} = 5.449$ .

Below  $\bar{t}_t$  there is a line of gas-liquid first order transitions induced by the magnetic interaction. In reference [13] the dependence of the difference between the volumes in the gas and the liquid phase on the coexistence curve,  $x_1 - x_2$ , on the distance  $\bar{t}_t - \bar{t}$  has been found to be  $x_1 - x_2 \propto \bar{t}_t - \bar{t}$  yielding the critical exponent  $\beta_2 = 1$ . Because of the magnetic coupling the critical properties of the fluid are different in the paramagnetic and the ferromagnetic phase. For the critical exponent of the volume,  $x_t - x \propto (\bar{p}_t - \bar{p})^{1/\delta_2}$ , the authors of reference [13] obtained  $\delta_2 = 2$  for  $x \rightarrow x_{t,-}$  and  $\delta_2 = 1$  for  $x \rightarrow x_{t,+}$ .

### 2.2.2 The phase diagram in an external magnetic field

In the complete phase diagram, including the magnetic field, the tricritical point is the origin of two lines of critical points  $L_+$  and  $L_-$  which border two surfaces of first order phase transitions, the so-called wings. In the limit  $\bar{h} \rightarrow \infty$  the magnetization approaches the maximum value  $m^2 = 1$  and the EOS has the simple van der Waals like form

$$\bar{p} = \frac{\bar{t}}{x-1} - \frac{1}{2x^2}; \quad (2.16)$$

the critical point ( $CP_{as}$ ) is the usual van der Waals critical point with the values (2.11) in the scaled fields

$$\begin{aligned} \bar{t}_{as} &= 4/27 = 0.148, \\ \bar{p}_{as} &= 1/54 = 1.852 \times 10^{-2} \end{aligned} \quad (2.17)$$

and  $x_{as} = 3$ . The temperature and pressure values of the tricritical point (2.15) are well above these values. The  $L_+$  line calculated below connects these points.

The conditions for the points on the line of second order transitions  $L_+$  are

$$\frac{\partial \bar{p}}{\partial x} = 0, \quad \frac{\partial^2 \bar{p}}{\partial x^2} = 0. \quad (2.18)$$

Inserting the derivative  $\partial m/\partial x$  obtained from the magnetic EOS (2.12) into these conditions one finds the magnetization  $m^2$  and the temperature  $\bar{t}$  as functions of  $x$  only

$$m^2(x) = \frac{x^2(6x - x^2 - 3)}{9x^2 - 10x + 3}, \quad (2.19)$$

$$\bar{t}(x) = \frac{2(x-1)^2}{9x^2 - 10x + 3}, \quad (2.20)$$

where  $x$  may vary between its two limiting values  $x_c$  and  $x_t$ :  $3 \leq x \leq 3 + \sqrt{6} = 5.449$ . One can easily convince oneself, that  $\bar{t}(x)$  and  $m^2(x)$  take the appropriate values for  $x_{as} = x_c$  (2.17) and  $x_t$  (2.15). From

$$\bar{h}(x) = \frac{1}{2} \bar{t}(x) \ln \frac{1+m(x)}{1-m(x)} - \frac{m(x)}{x} \quad (2.21)$$

one knows the magnetic field  $\bar{h}$ , and (2.13) gives the pressure as function of  $x$

$$\bar{p}(x) = \frac{\bar{t}(x)}{x-1} - \frac{m^2(x)}{2x^2}. \quad (2.22)$$

Together with (2.19, 2.20) these equations establish the parameter representation of the  $L_+$  line in  $(\bar{t}, \bar{h}, \bar{p})$ -space. The magnetic interaction together with the finite magnetization leads to this line of critical points. It is a line of second order gas-liquid transitions. The line  $L_-$  is the symmetric counterpart to  $L_+$ , see the complete phase diagram shown in Figure 1.

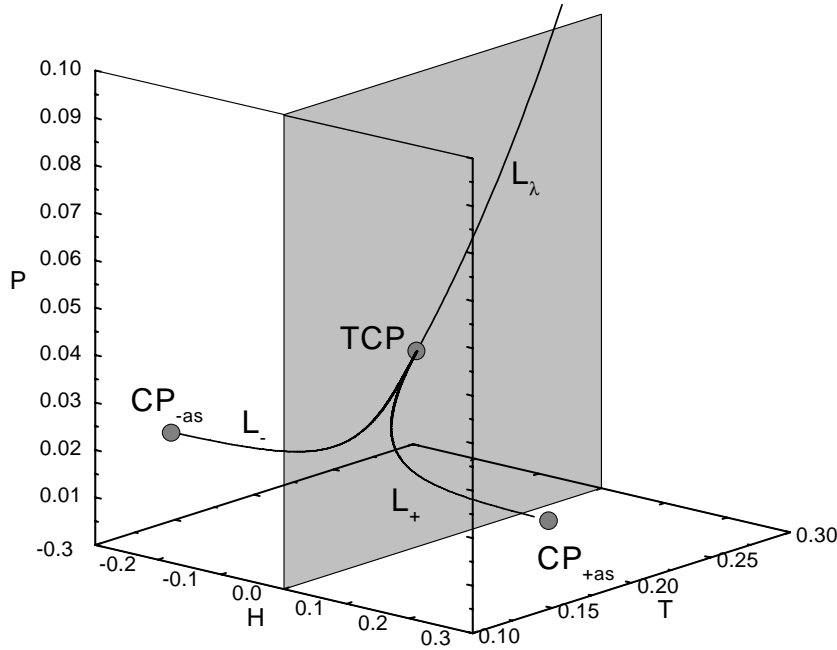


**Fig. 1.** Phase diagram ( $P$  pressure,  $T$  temperature,  $H$  magnetic field) for the ideal Ising fluid; only the critical lines are shown:  $L_\lambda$  is the line of second order magnetic transitions,  $L_+$  and  $L_-$  are the lines of second order gas-liquid transitions, the shaded surface indicates the  $H = 0$  plane. The filled circles mark the tricritical point (TCP) and the two asymptotic critical points ( $CP_{\pm as}$ ) at  $H \rightarrow \infty$ .

### Approaching the tricritical point along $L_\pm$

Expanding the parametric representation of  $L_\pm$  in  $\eta = x_t - x$  shows how these critical lines approach the tricritical point. In order to determine this behavior we investigate first the magnetization for  $h \rightarrow 0$ , *i.e.* in our parametrization we have to find  $m^2(x)$  for  $x \rightarrow x_t = 3 + \sqrt{6}$ . Performing in (2.19) the limit  $\eta \rightarrow 0$  gives

$$m^2(x_t - \eta) \simeq \frac{3}{2} (\sqrt{6} - 2) \eta = 0.674 \eta \quad (2.23)$$

so that we conclude

$$m \propto \eta^{1/2} = (x_t - x)^{1/2}. \quad (2.24)$$

For the temperature  $\bar{t}$  and the pressure  $\bar{p}$  we find from (2.20, 2.22) in the vicinity of  $x_t$  ( $\bar{t}_t = 1/x_t$ )

$$\bar{t}_t - \bar{t}_w(x_t - \eta) \simeq \frac{1}{6} (9\sqrt{6} - 22) \eta = 7.568 \times 10^{-3} \eta; \quad (2.25)$$

$$\bar{p}_t - \bar{p}_w(x_t - \eta) \simeq \frac{1}{12} (9\sqrt{6} - 22) \eta = 3.784 \times 10^{-3} \eta. \quad (2.26)$$

This means that on the critical line  $L_+$   $\bar{t}_t - \bar{t}_w$  and  $\bar{p}_t - \bar{p}_w$  are proportional to  $x_t - x$ .

A little bit more involved is the determination of  $\bar{h}(\eta)$  for  $\eta \rightarrow 0$  from (2.21) which should lead to the power law behavior  $\bar{h}(\eta) \propto \eta^\rho$  for  $\eta \rightarrow 0$  with some exponent  $\rho$ . Superficially equation (2.21) seems to yield  $\rho = 3/2$  but due to a cancellation of lower order terms the exponent is larger. Keeping the necessary powers of  $\eta$  and performing the limit  $\eta \rightarrow 0$  we find

$$\begin{aligned} \bar{h}(\eta) &\simeq \frac{2}{15} (89\sqrt{6} - 218) \eta^2 m(\eta) \\ &= 5.022 \times 10^{-4} \eta^{5/2}, \end{aligned} \quad (2.27)$$

hence  $\bar{h}(x) \propto (x_t - x)^{5/2}$ . Inserting the inverted relation

$$x(\bar{h}) = x_t - 20.876 \bar{h}^{2/5}. \quad (2.28)$$

into (2.23) yields the magnetic equation of state  $m \propto \bar{h}^{1/5}$  when approaching  $\bar{t}_t$  on one of the lines  $L_\pm$ ; thus for this direction [19] the critical exponent [20] is

$$\delta_t = 5. \quad (2.29)$$

Finally  $L_+$  for small magnetic fields  $\bar{h}$  is represented in a  $(t, p, h)$ -diagram by

$$\bar{t}_w(\bar{h}) = \bar{t}_t - 0.158 \bar{h}^{2/5} \quad (2.30)$$

$$\bar{p}_w(\bar{h}) = \bar{p}_t - 0.079 \bar{h}^{2/5}. \quad (2.31)$$

### In the vicinity of the wing critical point

For finite  $\bar{h}$  there is only the critical point on the  $L_\pm$ -line in the magnetized fluid. The finite magnetization brings about a density dependent contribution to the pressure. Due to this term there is now a “gas-liquid” critical point. In the limit of large magnetic fields this critical point is of van der Waals type. At finite  $\bar{h}$  we find for all phase transitions  $\gamma_- = \gamma_+ = 1$ . On the other hand, at the tricritical point the nature of the phase transition changes and the transition becomes a magnetic one. There the values of the exponent of the compressibility in the magnetically ordered phase,  $\gamma_- = 1$ , is different from the one in the disordered phase,  $\gamma_+ = 0$  [13].

## 2.3 The one dimensional Ising van der Waals fluid in an external magnetic field

Let us now return to the magnetic van der Waals gas. In the presence of a magnetic field we expect additional

critical lines: one which originates from the tricritical point (similar as in the ideal case) and, for certain values of  $R$ , one which originates from the critical point.

### 2.3.1 The equation for the critical lines

As before, the critical lines for  $h \neq 0$  (if they exist) are subject to the conditions  $\partial p/\partial x = 0$  and  $\partial^2 p/\partial x^2 = 0$ . These conditions contain *all* critical lines, the wing critical lines  $L_{\pm}$  and the ordinary gas-liquid critical line.

From the magnetic EOS (2.4) we have now  $\frac{\partial m}{\partial x} = \frac{m(1-m^2)}{x(1-m^2-xt/R)}$ . Inserted into the first condition for a critical point (compare (2.18)) we find

$$m^2 = \frac{(1-xt/R)((x-1)^2-xt^3)}{(x-1)^2-xt(2x-1)}. \quad (2.32)$$

and together with the second condition we get a cubic equation

$$\begin{aligned} z^3 - 2z^2 \frac{(Rx+6x-3)}{(9x^2-10x+3)} \\ + z \frac{(R(x^2+6x-3)+3(x^2+2x-1))}{x^2(9x^2-10x+3)} \\ - \frac{2(R+1)}{x^2(9x^2-10x+3)} = 0, \end{aligned} \quad (2.33)$$

for the variable  $z = xt/(x-1)^2$ .

For arbitrary values of  $h$  we have to resort to the equation (2.33). For each value of the inverse density  $x$  there are three solutions for the scaled temperature  $z_i(x)$ . The physical solutions have to fulfill several conditions: (i)  $z_i(x)$  has to be real, (ii) the magnetization squared

$$m^2(x, z_i(x)) = \frac{(1-(x-1)^2 z_i(x)/R)(1-z_i(x)x^2)}{1-z_i(x)(2x-1)}. \quad (2.34)$$

has to be positive and smaller than or equal to 1, (iii) the pressure  $p$  found from the EOS has also to be positive. Solutions, which do not fulfill condition (iii), are already in the region of the first order transition and the Maxwell construction takes care of the proper (positive) pressure.

These three conditions leave at most *two* physically meaningful real roots, which correspond to  $t_w(x)$ ,  $h_w(x)$ ,  $p_w(x)$  and  $t_c(x)$ ,  $h_c(x)$ ,  $p_c(x)$ . Depending on the topology of the phase diagram at  $h = 0$ , *i.e.* depending on the value of  $R$ , one of these two second order transition lines reaches the asymptotic critical point at  $t_{c,as}$ ,  $\infty$ ,  $p_{c,as}$ . The situation of this limiting case for  $h \rightarrow \infty$  is reached already for moderate values of  $h$ .

Varying the temperature the isotherms may show three types of saddle points: (i) a point related to  $L_{\pm}$  (see point  $CP_w$  in Fig. 2), (ii) one related to the line of critical points (see point CP in Fig. 2) and (iii) a virtual point (situated in the coexistence region) which results from the contribution of the increasing magnetization to the pressure (see the dot in Fig. 2).

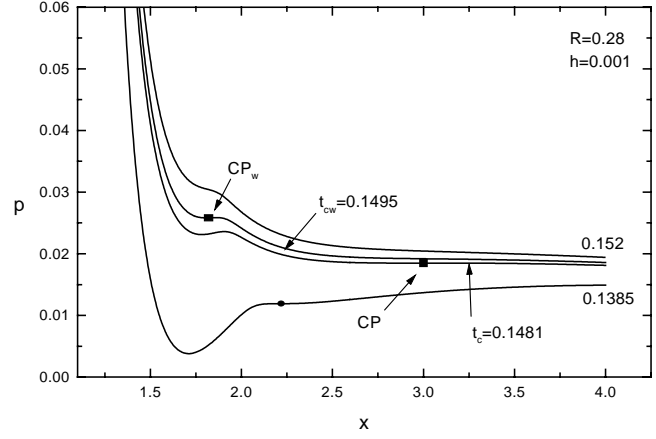


**Fig. 2.** Isotherms of the Ising van der Waals fluid at  $R = 0.28$  in the  $p - x$  diagram for finite  $h = 0.001$  without Maxwell construction. The squares mark the wing critical point ( $CP_w$ ) and the gas-liquid critical point (CP) on their respective critical isotherms. The dot marks a virtual critical point within the coexistence region of a first order gas-liquid transition.

For the limiting cases  $h \rightarrow \infty$  and close to the critical point at  $h = 0$  the transition temperatures can be found more directly. For three different cases of topology the second order phase transition lines determined from (2.33) are shown in Figures 3-5.

#### The limit of infinite strong magnetic field

In the limit  $h \rightarrow \infty$  the solution of the magnetic equation of state is  $m^2 = 1$  and consequently the equation for the pressure reduces to the simple van der Waals form

$$p = \frac{t}{x-1} - \frac{R+1}{2x^2},$$

whose only critical point has the coordinates

$$\begin{aligned} t_{c,as} &= \frac{4}{27}(R+1), \\ p_{c,as} &= \frac{1}{54}(R+1), \\ h_{c,as} &= \infty \end{aligned} \quad (2.35)$$

and  $x_{c,as} = 3$ . This means that equation (2.33) has only one physical solution in that limit.

#### The gas-liquid critical line in small fields

Near the critical point *i.e.* small values of  $h$  and  $R/xt < 1$  (in fact for  $R = 1/4$  we have  $R/x_c t_c = 9/16$  with (2.11))  $m$  is also small and therefore we may expand the magnetic EOS (2.4)

$$m = \frac{h}{t(1 - \frac{R}{xt})}. \quad (2.36)$$

$$a_y(R) = \frac{3R}{2} \frac{(9R^2 + 15R + 2)\sqrt{2R(3R+2)} - 2(3R+2)(3R^2 + 2R - 4)}{27R^3 + 54R^2 + 9R - 16}. \quad (2.40)$$

$$p_{hs}(\rho, T) = \begin{cases} T\rho \frac{1 + \rho^2 - 0.67825\rho^3 - \rho^4 - 0.5\rho^5 - 1.7\rho^6}{1 - 3\rho + 3\rho^2 - 1.04305\rho^3} & \rho \leq 0.4927 \\ p_{hs}(0.4927, T) & 0.4927 < \rho \leq 0.54447 \\ T\rho \frac{1 + \rho + \rho^2 - 0.67825\rho^3 - \rho^4 - 0.5\rho^5 - 6.028e^{\xi(7.9-3.9\xi)}\rho^6}{1 - 3\rho + 3\rho^2 - 1.04305\rho^3} & \rho > 0.54447. \end{cases} \quad (3.1)$$

and insert it into (2.5). From the two equations (2.18) we obtain then the critical values  $t_c(h)$  and  $p_c(h)$  in order  $h^2$

$$t_c(h) = \frac{4}{27} + \frac{16}{27} \frac{1}{\left(\frac{4}{9} - R\right)^3} Rh^2 \quad (2.37)$$

$$p_c(h) = \frac{1}{54} + \frac{1}{2} \frac{\frac{4}{27} + R}{\left(\frac{4}{9} - R\right)^3} Rh^2 \quad (2.38)$$

with  $x_c(h) = 3 - 24R^2h^2/\left(\frac{4}{9} - R\right)^4$ . Of course this discussion applies only for that range of values of the parameter  $R$  where the critical point at  $h = 0$  exists.

### 2.3.2 The lines $L_{\pm}$ near the tricritical point

In the vicinity of the tricritical point we may perform an expansion similar as in subsection 2.2.2 by setting

$$x = x_t - \eta \quad \text{and} \quad xt = R - a_y\eta \quad (2.39)$$

(note  $x_t t_t = R$ ). Inserted into equation (2.33) we get for  $a_y$

*see equation (2.40) above.*

In the limit  $R \rightarrow \infty$ , where  $a_y \rightarrow R(\sqrt{6} - 2)/2$ , we recover the result of the ideal Ising fluid. This can be verified from a comparison with equation (2.25) taking into account that  $a_y = (1/6)(9\sqrt{6} - 22)x_t + t_t$ .

Inserting the ansatz (2.39) for  $x$  and  $y$  into the magnetization (2.32) yields

$$m^2 = \frac{3a_y}{R}\eta \quad (2.41)$$

and from the magnetic EOS solved for the field (compare (2.21)) we get

$$h(x_t - \eta) = f(R)\eta^2\sqrt{a_y\eta} \quad (2.42)$$

with some function  $f(R)$ . Expanding also  $t_w$  and  $p_w$

$$\begin{aligned} t_w(x_t - \eta) &= t_t - \frac{a_y - t_t}{R/t_t}\eta, \\ p_w(x_t - \eta) &= p_t - \left(\frac{t_t}{R}\right)^2 \left(\frac{1}{2} \frac{5t_t - 3R}{t_t - R} a_y \right. \\ &\quad \left. - R^2 \frac{2t_t - R}{(t_t - R)^2} + \frac{t_t}{R}\right)\eta \end{aligned} \quad (2.43)$$

and inserting from (2.42)  $\eta(h)$  gives the parameter form of the wing edges  $L_{\pm}$

$$t_w(h) = t_t - a_t(R)h^{2/5} \quad (2.44)$$

$$p_w(h) = p_t - a_p(R)h^{2/5}. \quad (2.45)$$

For large  $R$  both  $a_t(R)$  and  $a_p(R)$  behave as  $R^{3/5}$  and thus one recovers equations (2.30, 2.31).

## 3 Phase diagram topologies for the Heisenberg fluid

Since we shall restrict ourselves to numerical calculations we can use an improved hard sphere contribution to the pressure more appropriate to the three-dimensional case than the van der Waals expression. The magnetic interaction is now of Heisenberg type. This means that we extend the calculations of [14] to finite magnetic fields. Strictly speaking we use for the hard sphere pressure instead of the Carnahan-Starling equation [21] the equations given by Hall [22] in the whole region of densities,

*see equation (3.1) above.*

For  $H = 0$  this does not lead to essential numerical differences to the results of [14].

The magnetic EOS for the isotropic classical Heisenberg model reads

$$m(\rho, T, H) = L\left(\frac{R\rho m}{T} + \frac{H}{T}\right) \quad (3.2)$$

with the Langevin function  $L(z) = \coth(z) - 1/z$ . Then the pressure reads

$$P(\rho, T, H) = \mathcal{MC} \left[ p_{hs}(\rho, T) - \frac{1}{2}R\rho^2 m(\rho, T, H) - \frac{1}{2}\rho^2 \right]. \quad (3.3)$$

$\mathcal{MC}$  indicates as before the Maxwell construction and  $\rho$ ,  $T$ ,  $p$  and  $H$  are measured in the units  $\pi b^3/6$ ,  $\pi b^3 k/(6a)$ ,  $(\pi b^3/6)^2/a$  and  $\pi b^3/a$  respectively.

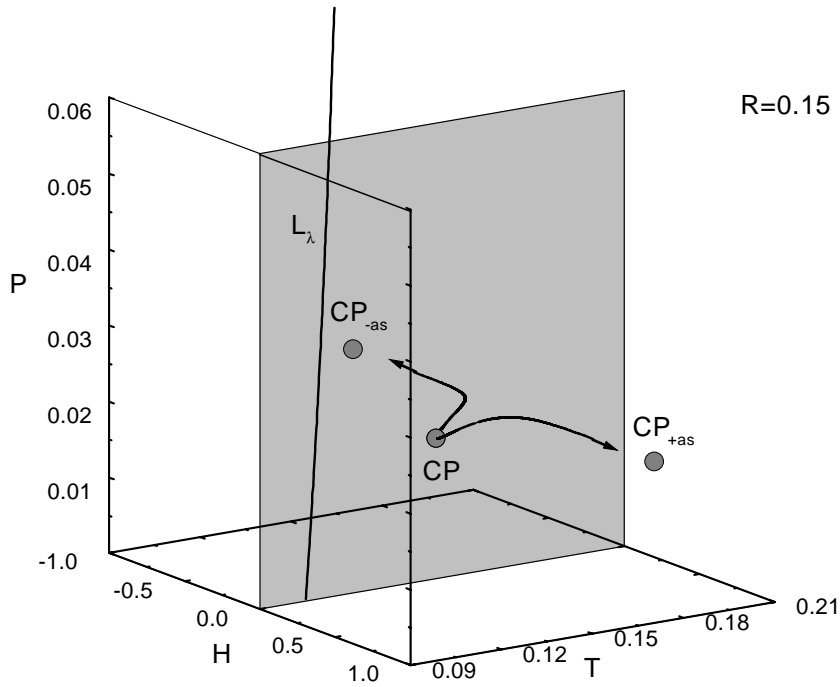


**Fig. 3.** Phase diagram of the Ising fluid in a magnetic field for  $R = 0.15$ ; only the lines of critical points are shown, symbols as in Figure 1.

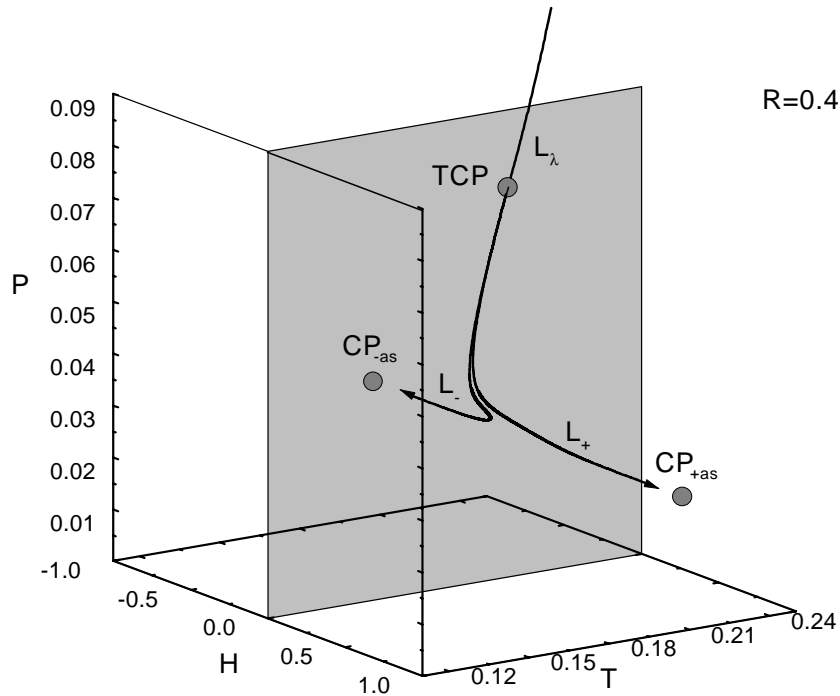


**Fig. 4.** Phase diagram of the Ising fluid in a magnetic field for  $R = 0.40$ ; only the lines of critical points are shown, symbols as in Figure 1.

### 3.1 Zero magnetic field

Hemmer and Imbro [14] have investigated systematically the possible topologies of the phase diagrams in the zero field case. For special values of the ratio  $R$  phase diagrams have been constructed by integral equation methods [6], density functional methods and computer simulations [8–11]. We show in Figure 6 those parts of the phase diagram as function of the ratio  $R$ , which contain the fluid phases and which have already been calculated in [14]. The first order surface of gas liquid phase transi-

tions (light gray surface) is limited on one side by a line of critical points (LCP) which in turn terminates in a critical end point (CEP) (there it touches the surface of first order phase transition between the paramagnetic gaseous and the ferromagnetic liquid phase (gray surface)). On the other side the surface meets the surface of magnetic transitions (hatched and gray surface) in a line which consists of two parts, critical end points (LCEP) and triple points (LTP).

The surface of magnetic phase transitions consists of two parts, the hatched part, where the second order

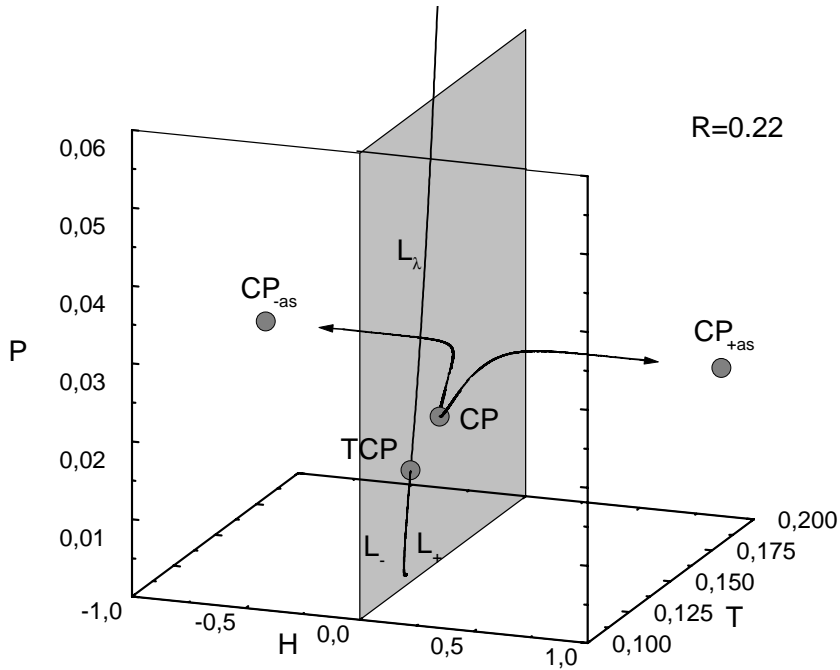


**Fig. 5.** Phase diagram of the Ising fluid in a magnetic field for  $R = 0.22$ ; only the lines of critical points are shown, symbols as in Figure 1.

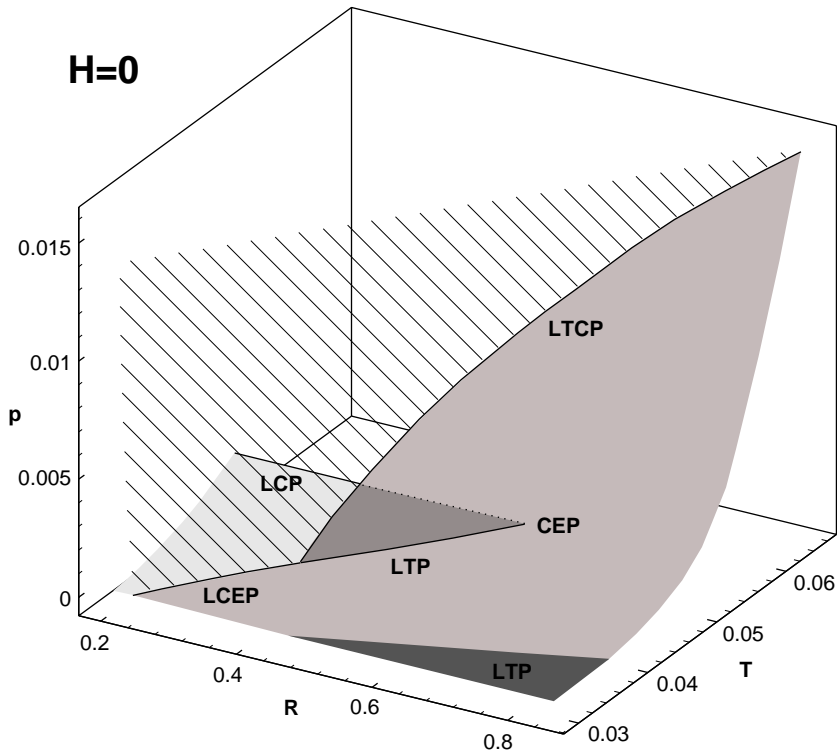


**Fig. 6.** Phase diagram in zero magnetic field as function of the ratio  $R$  of the magnetic interaction to the van der Waals interaction.  $P$  pressure, and  $T$  temperature. Lines of critical points (LCP), tricritical points (LTCP), critical endpoints (LCEP) and triple points (LTP) are present. The surface of second order magnetic transitions is hatched; all other surfaces indicate first order transitions: gas-liquid (light gray), paramagnetic-ferromagnetic liquid (gray), paramagnetic gas-ferromagnetic solid (dark gray).

transitions take place, and the gray part, where the transitions are of first order. The border between these two parts is the already mentioned line of critical end points (LCEP) and of tricritical points (LTP).

A second line of triple points (LTP, the intersection of the gray and dark surface) exists; there the surface of solid-liquid transitions (which is not shown) meets the surface of magnetic transitions (either liquid-liquid transitions (gray) or solid-gaseous transitions (dark gray)).

By crossing the surface of second order magnetic transitions (hatched surface) the density of the fluid changes continuously but with discontinuous derivative.

One of the interesting questions is whether computer simulations can verify this complicated topology, in particular the existence of the tricritical line LTCP. Since the tricritical point is not ruled out by computer simulations, other techniques have to be used to clarify this question [11]. It is known from other examples [23] that fluctuations



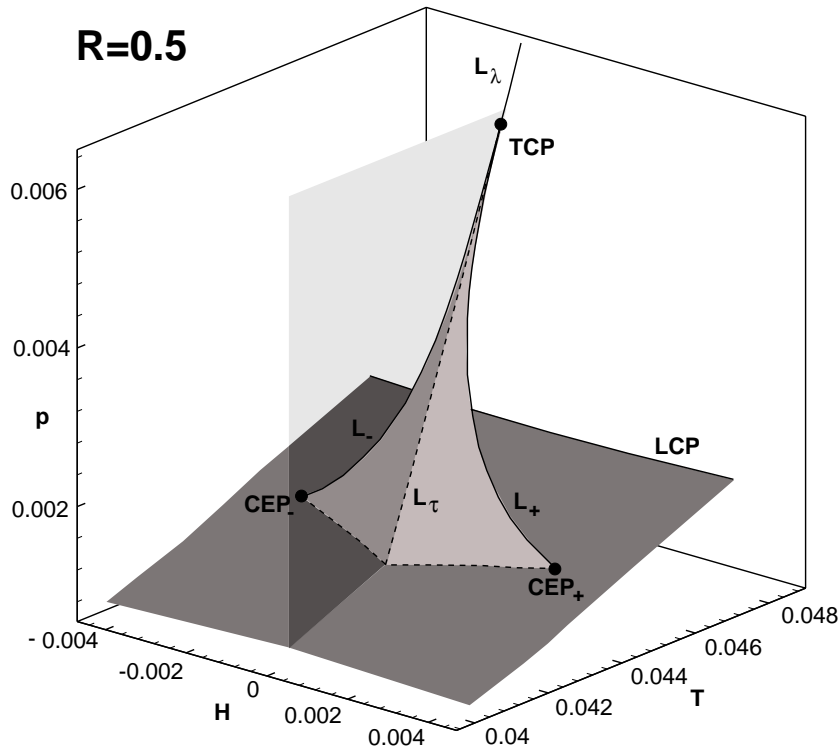


**Fig. 7.** Phase diagram of a Heisenberg fluid for  $R = 0.5$ .  $P$  pressure,  $H$  magnetic field,  $T$  temperature. Second order lines are solid:  $L_\lambda$  (magnetic critical points),  $L_\pm$  (liquid-liquid critical points), LCP (gas-liquid critical points). Dashed lines are lines of triple points. The various planes indicate first order transitions: opaque plane (magnetic transitions), light gray planes (liquid-liquid transitions), dark gray plane (gas-liquid transitions). The dots indicate multicritical points: TCP (tricritical point),  $CEP_\pm$  (critical end points).

may shift regions of first and second order transitions in the field space, thus it is possible that the extension of the LTCP-line is reduced in favor of the LCEP-line, accompanied by an increase of the hatched second order surface.

### 3.2 Finite magnetic field

In order to have more information on the mean field topology of the phase diagrams we extend the space of fields including the magnetic field  $H$ . One effect is of course that the magnetic phase transitions disappear, however the contributions of the finite magnetization to the pressure change the properties of the Heisenberg fluid and besides the gas liquid transition an additional phase transition in the fluid may appear similar to the Ising interaction. From the variety of topologies of phase diagrams we consider first the situation where at zero field a tricritical as well as a critical point exists. This is the case for  $R = 0.5$  (see Fig. 7). From the tricritical point (TCP) at  $H = 0$  two lines of second order liquid-liquid transitions,  $L_\pm$ , emerge. They are the border lines of surfaces of first order transitions (called wings, gray) adjoining in lines of triple points (dashed) the surface of first order gas-liquid transitions (dark gray). The points on the line  $L_\tau$  where the magnetic first order surface at  $H = 0$  (light gray) meets the wings are triple points. At  $H = \pm 0.0031$ ,  $T = 0.044$  and  $P = 0.060$  the wing lines  $L_\pm$  impinge on the first order surface of the gas-liquid transitions. These points are critical end points ( $CEP_\pm$ ).

Decreasing  $R$  the wings become smaller. Finally, *e.g.* for  $R = 0.25$ , at  $H = 0$  no tricritical point exists, and the magnetic second order transition line  $L_\lambda$  terminates

in a critical end point (CEP) on the first order transition surface of gas-liquid transitions (dark gray) (see Fig. 8). The line of gas-liquid critical points (LCP) borders this surface of first order transitions.

In Figure 9 we present the phase diagram for different values of  $R$ . It shows the folded surface of first order phase transitions in the liquid. The line of critical points (LCP) and the line of wing critical points (LWCP) both terminate in critical end points (CEP) when they meet the first order transition surface (dark gray). The critical endpoints are connected by a line of triple points (LTP).

## 4 Discussion

Fluctuations may change the topology of a phase diagram as well as critical exponents from classical to non classical values. In the magnetic liquid this holds for the second order phase transitions, whereas at the tricritical point classical exponents are correct apart from logarithmic corrections to the power laws. As far as the topological features (number and positions of critical points and lines) are concerned, Monte-Carlo calculations and calculations in an extended mean field theory give qualitatively the same picture as the mean field calculations of reference [14] although the existence of a tricritical point is still under discussion [6, 8, 11] in three-dimensional systems. This is not the case in two dimensional magnetic fluids [3–5]. Also Monte-Carlo calculations indicate non classical exponents.

In the case of the Heisenberg fluid one expects the same values for the exponents as for the solid Heisenberg magnet, however small but significant differences have been

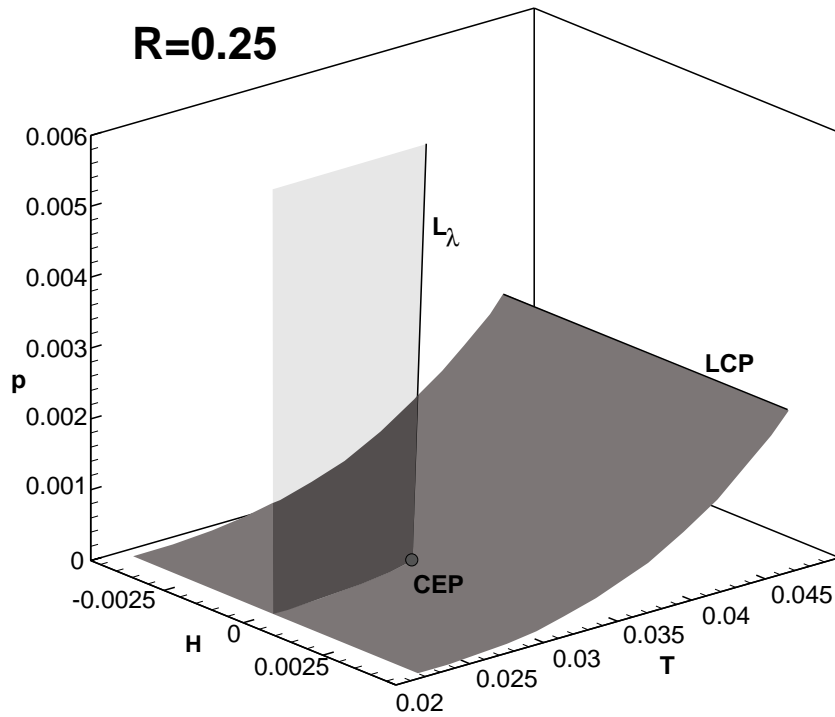


**Fig. 8.** Phase diagram for  $R = 0.25$ . the notation is the same as in Figure 7.

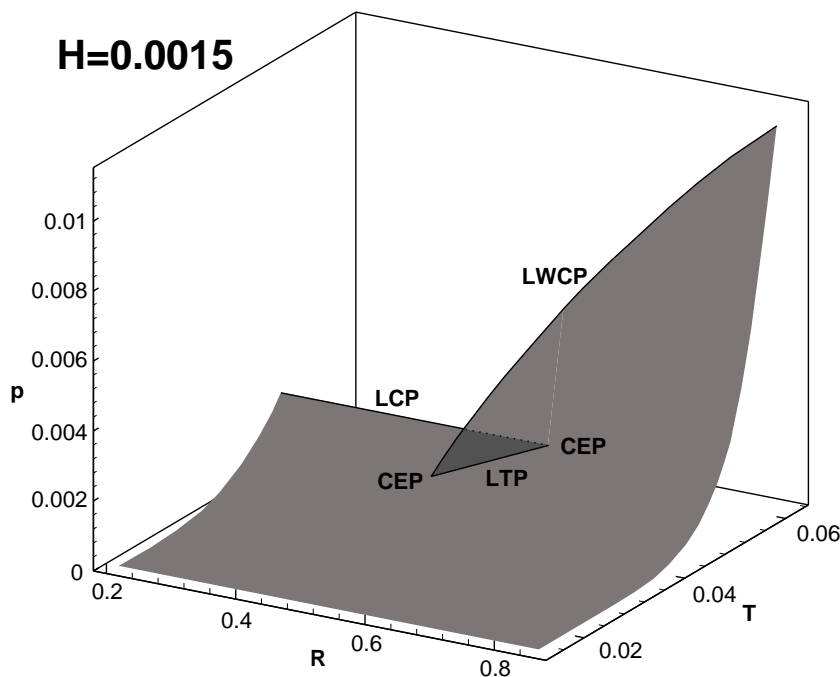


**Fig. 9.** Phase diagram of a Heisenberg fluid at  $H = 0.0015$  as function of the ratio  $R$ . The surface of first order transitions in the fluid (dark gray) is bordered by lines of critical points: the line of gas-liquid critical points ( $LCP$ ) and the line of wing critical points ( $LWCP$ ). The line of triple points ( $LTP$ ) terminates in critical endpoints ( $CEP$ ). Observe the branching of the surface at this line.

observed [9,10]. For the Ising fluid Fisher renormalized exponents [24] are expected because of the diverging specific heat, but there also deviations are observed [12]. It is not completely clear whether these deviations are due to non asymptotic (crossover) effects and/or finite size effects.

The study of magnetic liquids in finite magnetic fields can contribute to the clarification of these questions. In particular for the existence of the tricritical point at zero magnetic field can be corroborated by the verification of

the topology in finite magnetic field, especially the existence of the wings.

Further it seems to be worthwhile to look for the Fisher renormalization also in the case of the gas-liquid transitions in finite magnetic field. These transitions belong to the universality class of the Ising model [17] irrespectively of the type of the magnetic interaction and therefore one also expects Fisher renormalized exponents. In addition the verification of the existence of the critical endpoint on the first order gas-liquid surface is of interest.

Quite recently in reference [25] the symmetric binary fluid mixture with equal numbers of particles in both components on average has been considered in mean field theory as well as using Monte-Carlo simulation. This system can be mapped onto the Ising magnetic fluid model in zero magnetic field. The tricritical point, predicted by mean field theory, has been confirmed by Monte-Carlo simulations. Although the quantitative picture of the phase diagram remains inclusion of fluctuations shifts the numerical values of the phase transition temperatures and the regions of the parameter values of  $R$  for the different topologies of the phase diagram.

We thank A. Parola for sending us reference [12] prior to publication. We also acknowledge support by the Fonds zur Förderung der Wissenschaftlichen Forschung, F.S. under contract 11557, R.F. and H.I. under project 12422-TPH. This work is dedicated by R.F. and H.I. to Prof. F. Schwabl on the occasion of his 60th birthday.

## References

1. G. Brush, H.J. Guentherodt, Phys. Lett. A **27**, 110 (1968).
2. B. Kraft, H. Alexander, Phys. Kondens. Mat. **16**, 281 (1973).
3. P. de Smedt, P. Nielaba, J.L. Lebowitz, J. Talbot, Phys. Rev. A **38**, 1381 (1988).
4. D. Marx, P. Nielaba, K. Binder, Phys. Rev. Lett. **67**, 3124 (1991).
5. D. Marx, P. Nielaba, K. Binder, Phys. Rev. B **47**, 7788 (1993).
6. E. Lomba, J.J. Weis, N.G. Almarza, F. Bresme, G. Stell, Phys. Rev. E **49**, 5169 (1994).
7. M.J. Stevens, G.S. Grest, Phys. Rev. E **51**, 5976 (1995).
8. J.M. Tavares, M.M. Telo de Gama, P.I. Teixeira, J.J. Weis, M.J. Nijmeijer, Phys. Rev. E **52**, 1915 (1995).
9. M.J. Nijmeijer, J.J. Weis, Phys. Rev. Lett. **75**, 2887 (1995).
10. M.J. Nijmeijer, J.J. Weis, Phys. Rev. E **53**, 591 (1996).
11. J.J. Weis, M.J. Nijmeijer, J.M. Tavares, M.M. Telo de Gama, Phys. Rev. E **55**, 436 (1997).
12. M.J. Nijmeijer, A. Parola, L. Reatto, Phys. Rev. E **57**, 465 (1998).
13. N.E. Frankel, C.J. Thompson, J. Phys. C: Solid State Phys. **8**, 3194 (1975).
14. P.C. Hemmer, D. Imbro, Phys. Rev. A **16**, 380 (1977).
15. I.D. Lawrie, E. Sarbach in *Phase Transitions and Critical Phenomena*, edited C. Domb, J.L. Lebowitz (Academic Press, London 1984), Vol. 9.
16. We follow the notation of [15] in defining the exponents. Using the standard example of an antiferromagnet in a magnetic field the correspondence is the following: the alternating magnetization  $M^\dagger$ , the staggered field  $H^\dagger$ , the magnetization  $M$  and the magnetic field  $H$  correspond here to the magnetization  $m$ , the magnetic field  $H$ , the density  $\rho$  and the pressure  $p$ . The exponents are defined as in Table 1 of [15].
17. C. Domb, *The Critical Point* (Taylor & Francis, London, 1996).
18. L. Feijoo, C.W. Woo, Phys. Rev. B **22**, 2404 (1980).
19. In general approaching the critical line  $L_\lambda$  one may expand (2.12) up to third orders in  $m$  yielding  $m \propto \bar{h}^{1/\delta}$  with  $\delta = 3$ .
20. Contrary to [15] we introduced  $\delta_t$  in order to discriminate it from  $\delta$  valid along the second order magnetic transition line.
21. N.F. Carnahan, K.E. Starling, J. Chem. Phys. **51**, 635 (1969).
22. K. Hall, J. Chem. Phys. **57**, 2252 (1972).
23. A. Aharony, D. Blankshtein, in *Multicritical Phenomena*, edited by R. Pynn, A. Skjeltorp (Plenum Press, New York 1984).
24. M.E. Fisher, Phys. Rev. **176**, 257 (1968).
25. N.B. Wilding, F. Schmid, P. Nielaba, Phys. Rev. E **58**, 2201 (1998).